Main aspects of deformation and rock support in Norwegian road tunnels

A.H. Høien[a,b,*], B. Nilsen[a], R. Olsson[c]

[a] *Norwegian University of Science and Technology, Sem Sælands veg 1, 7491 Trondheim, Norway*
[b] *Norwegian Public Roads Administration, Postboks 8142 Dep, 0033 Oslo, Norway*
[c] *Norwegian Geotechnical Institute, PO Box 3930 Ullevaal Stadion, 0806 Oslo, Norway*

ABSTRACT

The general geology of Norway makes most of its tunnels to be constructed mainly in strong rock intersected by weakness zones of different sizes and characteristics. The Norwegian support tradition is, to the largest degree as possible, to reinforce the rock to make it self-bearing. In weak rock, this reinforcement has been accomplished by using bolts, sprayed concrete and ribs of reinforced concrete (RRS). RRS are normally designed with 6 rebars mounted on brackets that are attached to rock bolts with a center to center distance of 1.5 m covered in sprayed concrete. The spacing between the RRS in the tunnel direction is usually 1–3 m. In recent years, the application of RRS has gradually changed from following the blasted tunnel profile that formed unarched RRS that reinforced the rock to using RRS with an arched design that supports the rock. Following this development was an increase in the use of materials, as the amount of sprayed concrete used is now considerably larger and the rebar diameter changed from 16 to 20 mm. This change has also caused an abrupt increase in the support measures used for decreasing rock quality, from simple reinforcement by bolts and sprayed concrete to load-bearing arches. The authors believe that a more gradual transition is logical and this article will discuss and evaluate the current Norwegian support strategy by reviewing international theory, performing parameter analysis and presenting data from current and previous Norwegian road tunnels, with a focus on rock mass quality and deformations. It is concluded that arched RRS is not necessary for all cases where it is used today, and that evaluation of the need for load bearing arched RRS should be based on deformation considerations. Norwegian conditions comprise the basis for the discussion, but the problem at hand is also of general interest for hard rock tunnelling conditions.

1. Introduction

In Norwegian tunnelling, stability challenges are usually related to zones of weak rock. Typical challenges can include wide weakness zones in sub-sea fjord crossings 100–300 m (m) below sea level, minor zones and jointed rock in urban areas with typically a 5- to 100-m overburden, overstressing of solid rock and weakness zones for tunnels under high mountains or along steep valley sides (up to a 1000-m overburden or more). Many weakness zones include the remains of Mesozoic weathering and may contain swelling minerals.

The Norwegian tradition is to take advantage of the self-bearing capacity of the rock mass as much as possible. When rock reinforcement requires more than bolts and sprayed concrete, a lean support construction is used to reinforce and keep the rock mass in place, rather than heavy support constructions, for example, fully casted lining. This lean support is usually comprised of reinforced ribs of sprayed concrete (RRS) (see Fig. 1). The RRS is combined with spiling bolts and sprayed

concrete to keep the rock in place after blasting, before RRS installation. The spiling bolts are held in place in the rear end with either steel straps and radial rock bolts or RRS.

RRS typically consists of six rebars c/c 10 cm mounted to rock bolts c/c 1,5 m along the tunnel periphery and covered with sprayed concrete. Originally, the rebars were installed so that they strictly followed the blasted tunnel profile (unarched RRS; see Fig. 2a), but in recent years the practice for road tunnels in Norway has been to form load-bearing arches (arched RRS, Fig. 2b) (Pedersen et al., 2010).

The support of Norwegian road tunnels up to 2010 was basically decided subjectively on-site for each blast round, whilst after 2010, the Q-system (Barton et al., 1974) has been used to register rock mass quality and the support determined based on using a support table (see Section 5.2). As a result of the development of sprayed concrete with possibility of spraying thick layers of alkali-free accelerator, support of weak rock based on spiling bolts and/or RRS was developed in the 1990s (Holmøy and Aagaard, 2002). Support based on RRS since then

Fig. 1. Mounting of rebars for two RRS for permanent support (2). Further toward the face two (1) blast rounds are temporarily supported with spiling bolts held in place by steel straps and radial rock bolts. Finished RRS can be seen to the right (3).
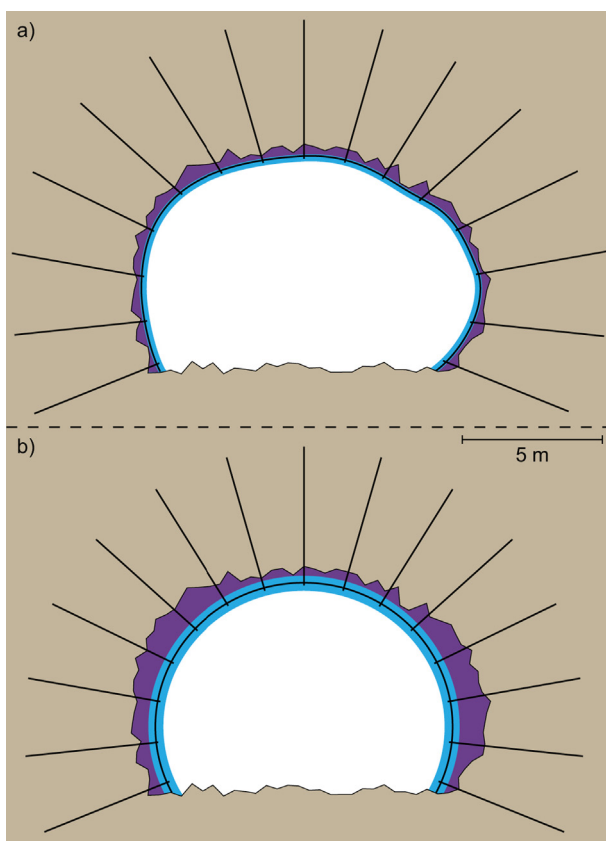

Fig. 2. Schematics of (a) unarched RRS and (b) arched RRS. The black lines are rebar and rock bolts. The purple area is sprayed concrete smoothing layer and the light blue area is the final layer covering the rebar. The rugged surface represents the blasted profile. (For interpretation of the references to colour in this figure legend, the reader is referred to the web version of this article.)

has slowly replaced the previously most common support of weak rock represented by cast concrete lining. A main reason for this is that RRS combined with spiling bolts enables much faster excavation than cast in place concrete lining, where one has to install a cast frame and wait for the concrete to harden. Support based on RRS was introduced in the Q-system in 2002 (Grimstad et al., 2002), and since 2010 arched RRS has been the main support measure for weak rock in road tunnels (Statens

vegvesen, 2010) while cast concrete lining has been used in only exceptional cases. Details of the combined excavation and support process based on using RRS are described in NFF (2008) and Pedersen et al. (2010).

The main purpose of this article is to discuss and evaluate the current support strategy focusing on rock mass quality and deformations. The current strategy involves a very considerable, abrupt increase of the support level at a certain drop in rock mass quality, from simple reinforcement with rock bolts and sprayed concrete to load-bearing constructions, such as arched RRS. It is believed that a more gradual transition from rock bolts and sprayed concrete to load-bearing support would be logical, and in this article the authors want to discuss and evaluate this possibility.

To create a basis for the discussion and evaluation, basic theories and international experiences will be reviewed. Data on rock mass quality, rock support and deformation in Norwegian tunnels, combined with a parameter study, will be used to illustrate the feasibility of a proposed alternative support strategy. The alternative approach addresses situations where the main challenge is local gravitational loading problems related to weak rock mass, filled joints, minor weakness zones and/or moderate swelling problems under favourable stress conditions. Norwegian geological conditions are typical for hard rock tunnelling and it is therefore believed that the conclusions of this study also will be of general interest for tunnelling in hard rock conditions.

2. Basic characteristics of Norwegian bedrock

2.1. Brief geological overview

Geologically, Norway mainly consists of Precambrian and Cambro Silurian (Caledonian) bedrock (see Fig. 3). The Precambrian rocks are mainly gneisses and intrusive granite and gabbro of various degrees of metamorphism. The Caledonian rocks are mainly metamorphosed sedimentary and volcanic rocks. Permian volcanic and igneous rocks can be found in Southeast Norway i.e. the Oslo region. In the Mesozoic, there was a weathering of bedrock that eroded during glacial landscape formation in the Pleistocene. The bedrock today therefore mainly consists of hard rock intersected by weakness zones of different extents and character originating from tectonic activity and in some cases, Mesozoic weathering.
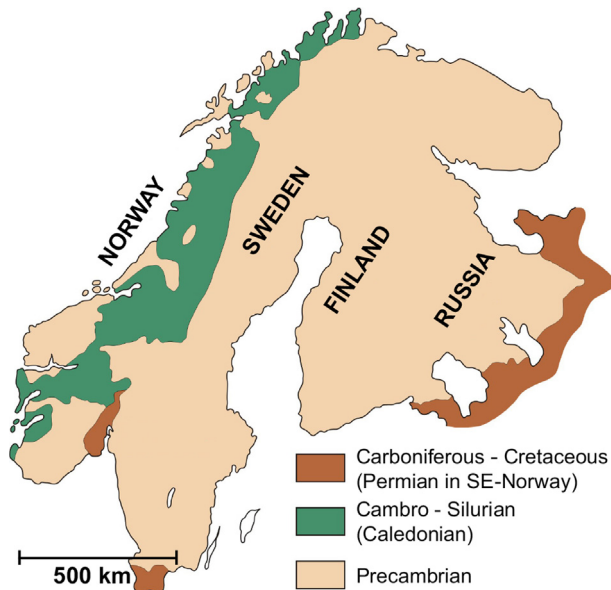
Fig. 3. Overview of regional geology.

2.2. Properties of intact rock

Box plots of uniaxial compressive strength (UCS) and E-modulus based on the SINTEF rock mechanical properties database (SINTEF, 2016) are shown in Figs. 4 and 5, respectively. The circles and stars are outliers and were not included in the distribution calculation. The dataset is based on testing about 3300 samples. There is considerable variation in both the UCS and the E-modulus but according to NBG (1985) classification, both the UCS and E-modulus values are large or very large.

2.3. Rock stresses

As for many other regions in the world, the in-situ rock stresses in Norway vary considerably in magnitude as well as orientation.

Myrvang (2001) stated that when measured, the horizontal stresses are usually much higher than the vertical component would indicate. He also stated that the vertical stress in most cases corresponds well to the overburden and is normally the minor principal stress, at least down to 500 m. An overview map of Norwegian geology and horizontal stresses is shown in Fig. 6. According to Myrvang (1993), the overall tendency is that the principal stresses seems to be parallel the Caledonian mountain range.

3. Theoretical basis for evaluating tunnel deformation and rock support

In this section, the pertinent background material on tunnel deformation and rock support will be presented. This material will be used in the subsequent main sections to evaluate current practices in Norwegian road tunnelling. As an important part of this evaluation, innovative application of the critical strain concept based on applying the SINTEF data presented in Section 2.2 is included for analysing how typical hard rock conditions will behave when affected by stresses.

3.1. Deformations from tunnel advancement

As the tunnel face advances, deformations take place in the rock mass. According to Hoek et al. (1997), the deformation starts about one-half of the tunnel diameter ahead of the face and at the face about one-third of the deformations have taken place. At about one to one and a half tunnel diameters behind the face, the deformations have reached their final value. This is confirmed by the results from RS3-modelling, based on the ideal conditions shown in Fig. 7. The model has the same conditions as the models described in Section 4, with 500 m overburden and the "GSI 50" material.

3.2. Critical strain

The critical strain concept was introduced by Sakurai (1981) and can be explained as the strain of a rock or rock mass at yield load. More specifically, the critical strain, ε_0, is:
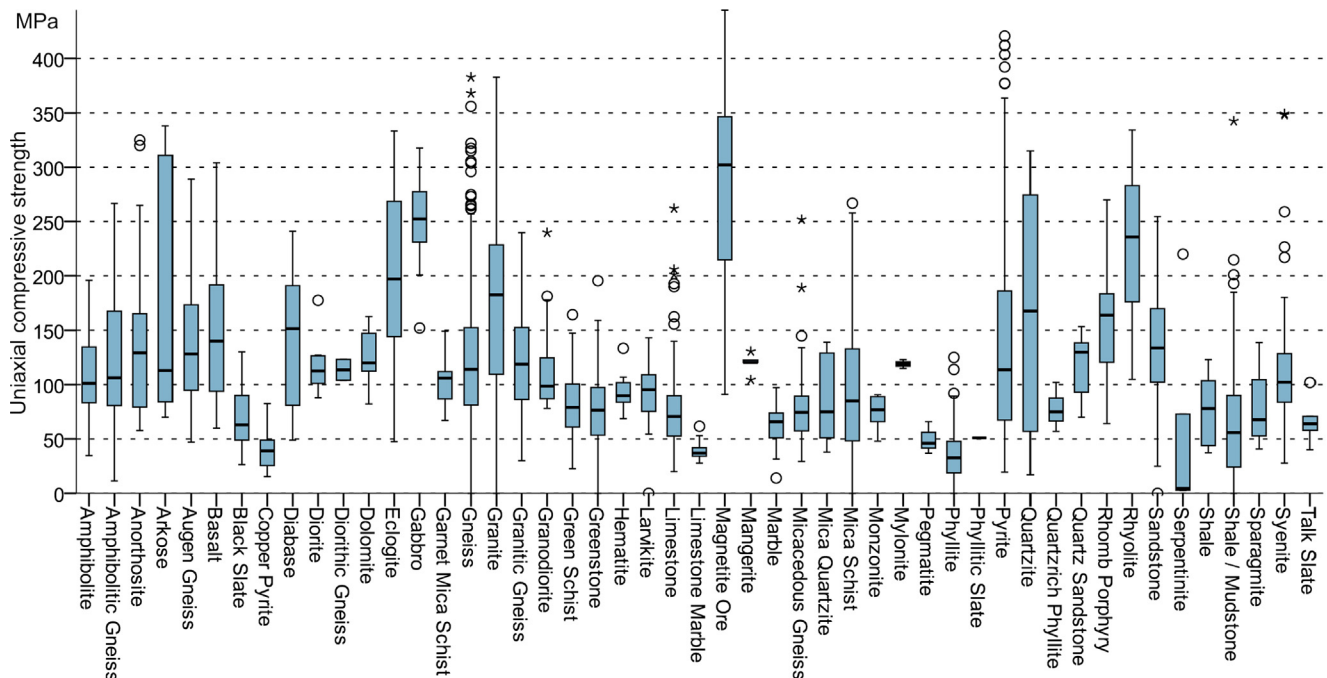

Fig. 4. Uniaxial compressive strength (UCS) in MPa for Norwegian rock types extracted from the SINTEF rock mechanical properties database (SINTEF, 2016).
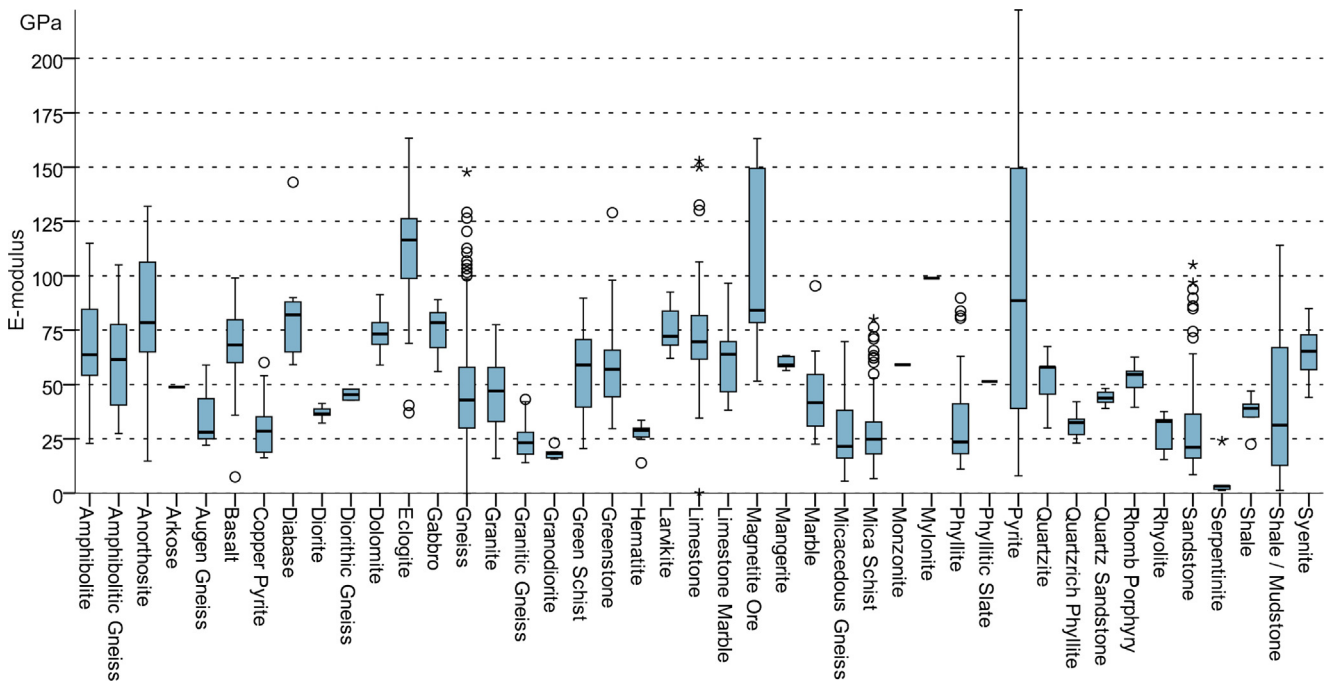
Fig. 5. E-modules in GPa for different Norwegian rock types extracted from the SINTEF rock mechanical properties database (SINTEF, 2016).
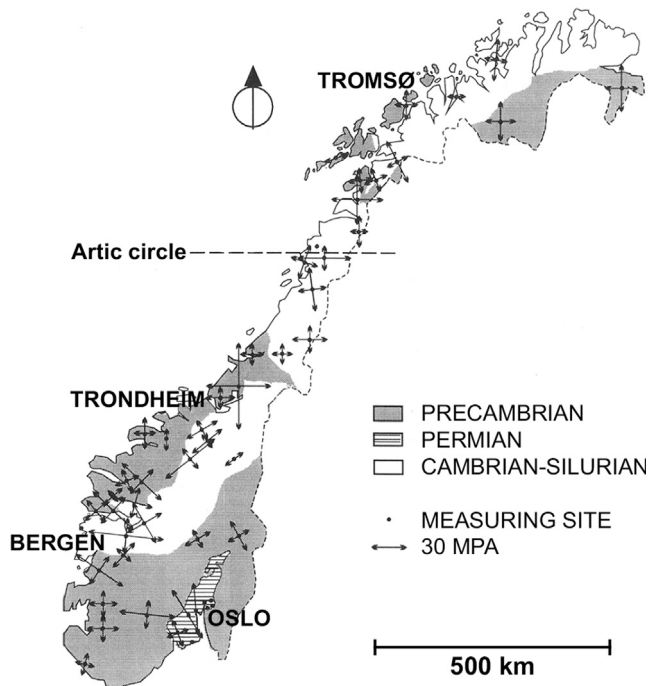

Fig. 6. Directions of horizontal stress in Norway (Myrvang, 1993).

$$\varepsilon_0 = \frac{\sigma_c}{E} \tag{1}$$

where σ_c is the UCS and E is the E-modulus.

For a linear elastic rock sample, critical strain would be the strain at maximum load during testing. Sakurai (1983) stated that the stability of tunnels can be assessed on the basis of strain in the rock mass surrounding the tunnel and showed how displacement measurements can be used in back-analysis to evaluate tunnel stability and initial stresses.

In Fig. 8, Sakurai's relationship between critical strain and uniaxial strength is presented with data for Norwegian rocks based on the SINTEF rock mechanical properties database (SINTEF, 2016). The red

lines in the figure envelope a large number of rock and soil core specimen tests, ranging from UCS 0.01 to 100 MPa, presented by Sakurai (1981). As illustrated, the critical strain tends to increase with the decrease of uniaxial compressive strength and ranges, according to Sakurai (1983), from 0.1% to 1% for rocks and from 1% to 5% for soil.

Based on in-situ testing and back-calculations, the critical strains for the rock mass of different rock types were derived (Sakurai, 1983). In Fig. 8, these relationships are shown where the grey line connects the corresponding core and rock mass values. The mean values obtained from core testing of corresponding Norwegian rock types (SINTEF, 2016) are presented as unfilled symbols in the same colour as Sakurai's data. A box plot of critical strains for Norwegian rock samples, based on the SINTEF-database (SINTEF, 2016), is presented in Fig. 9. One can see that most rock types have quite low critical strains, but since they have high UCS values, they can be exposed to significant stresses without reaching their limit.

3.3. Deformations related to rock mass strength and in-situ stress

In Hoek (1999), Hoek and Marinos (2000) and Hoek (2001), it is shown that strain and deformation can be predicted by the rock mass strength and in-situ stresses (see Fig. 10). Different classes are defined with a brief suggestion on how to reinforce or support rock, where the transition between typical rock reinforcement and rock support is between class A and B. The diagram is the result of a study on a closed formed analytical solution for a tunnel in a hydrostatic stress field, based on the theory of Duncan Fama (1993) and Carranza-Torres and Fairhurst (1999). A statistical simulation using the Monte Carlo method was conducted before a line fitting was performed on the data. The input values for the simulation were: in-situ stresses from 2 to 20 MPa (80–800 m depth), tunnel diameters from 4 to 16 m, uniaxial strength of intact rock from 1 to 30 MPa, Hoek-Brown constant m_i from of 5 to 12, Geological Strength Index (GSI) from 10 to 35 and, for the Carranza-Torres solution, a dilation angle of 0 to 10 (Hoek and Marinos, 2000).

Sakurai (1983) suggested that tunnel strain levels in excess of approximately 1% are associated with tunnel stability problems. This is supported by the plot in Fig. 11 (from Hoek (2001), where field observations of rock mass uniaxial strength are plotted against tunnel strain and observations are marked in red if they required special
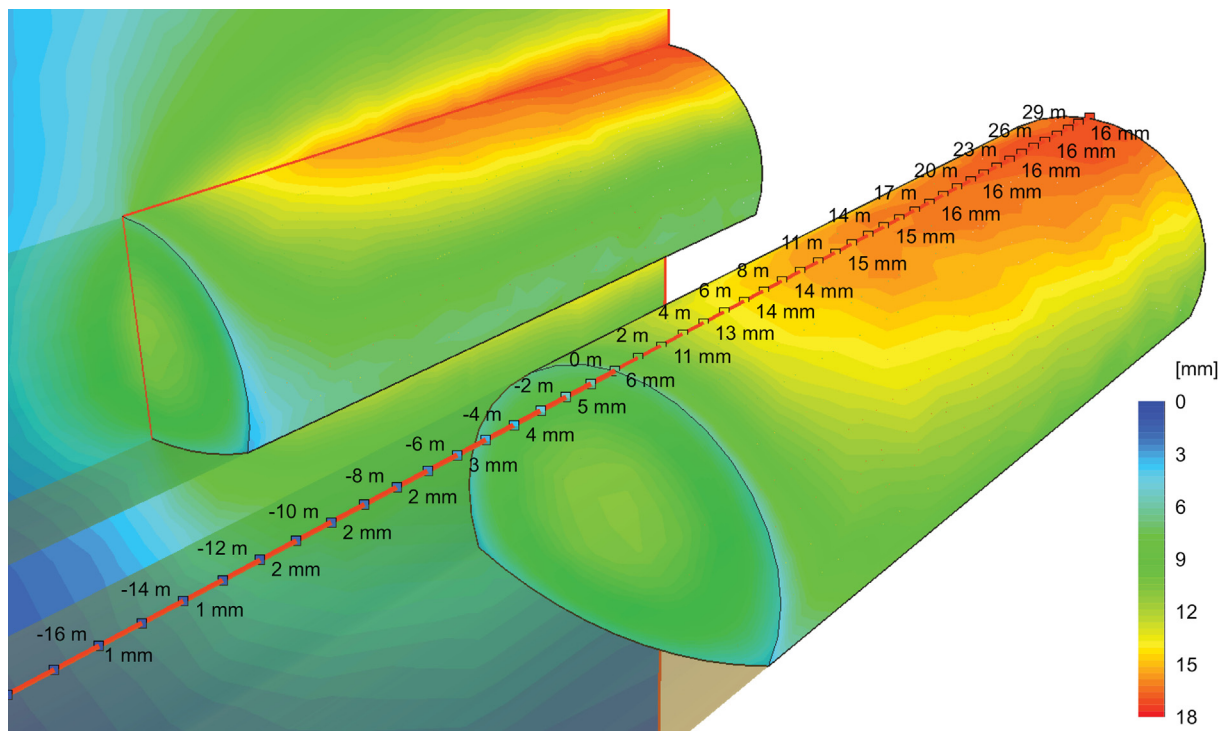
Fig. 7. Deformations around a typical two-tube tunnel (tube width is 10.5 m). Negative values are the meters in front of the face and positive values are the meters behind the face. The left tube has a vertical contour plane intersecting the centre of the tunnel.
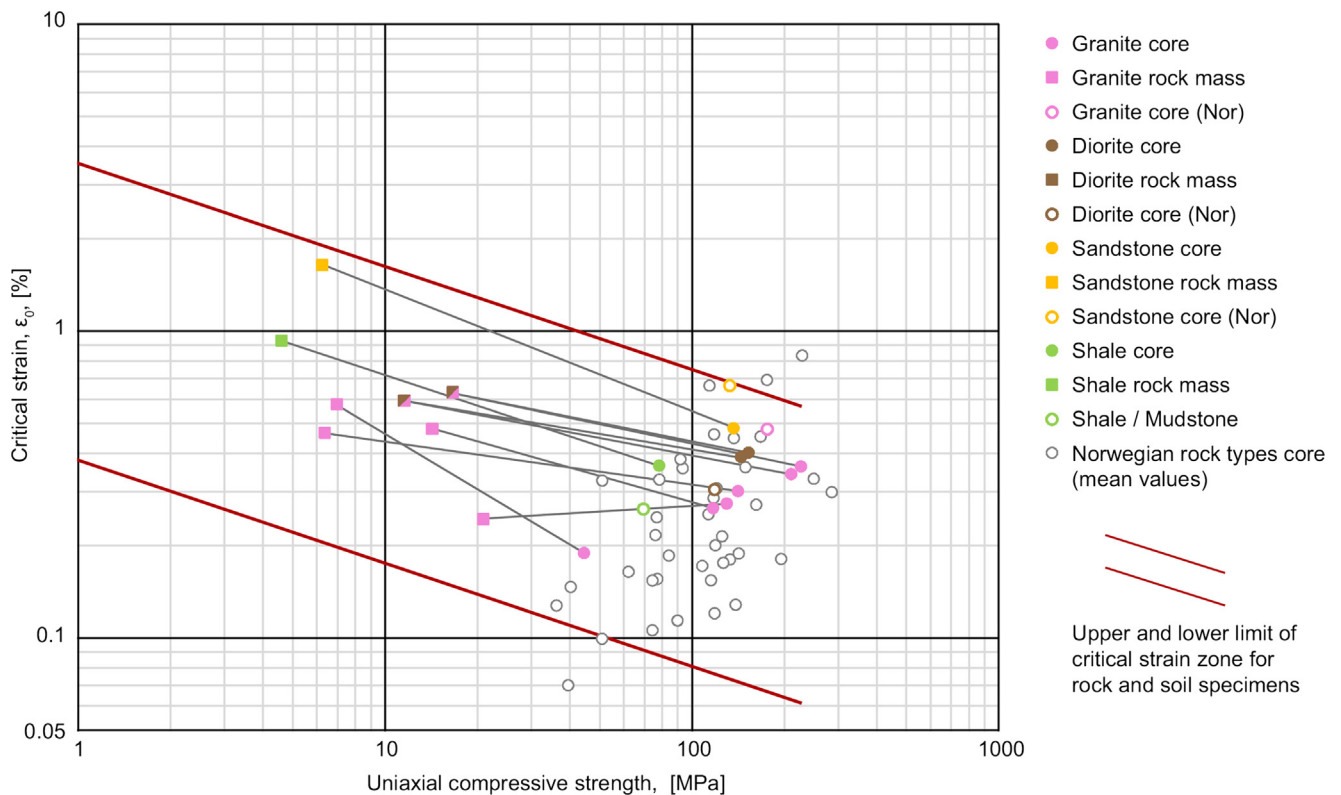
Fig. 8. Critical strains for rock cores and rock masses. The colour-filled symbols are data from Sakurai (1983), while the unfilled symbols are data from SINTEF (2016). The SINTEF values are the mean values for a certain rock type. The red lines are the envelope of an extensive number of tests on cores from Sakurai (1981). (For interpretation of the references to colour in this figure legend, the reader is referred to the web version of this article.)

Fig. 9. Critical strains for Norwegian rock types (SINTEF, 2016).

Fig. 10. The relationship between strain and rock mass strength and in-situ stress. The curve is for unsupported rock. Based on Hoek and Marinos (2000).

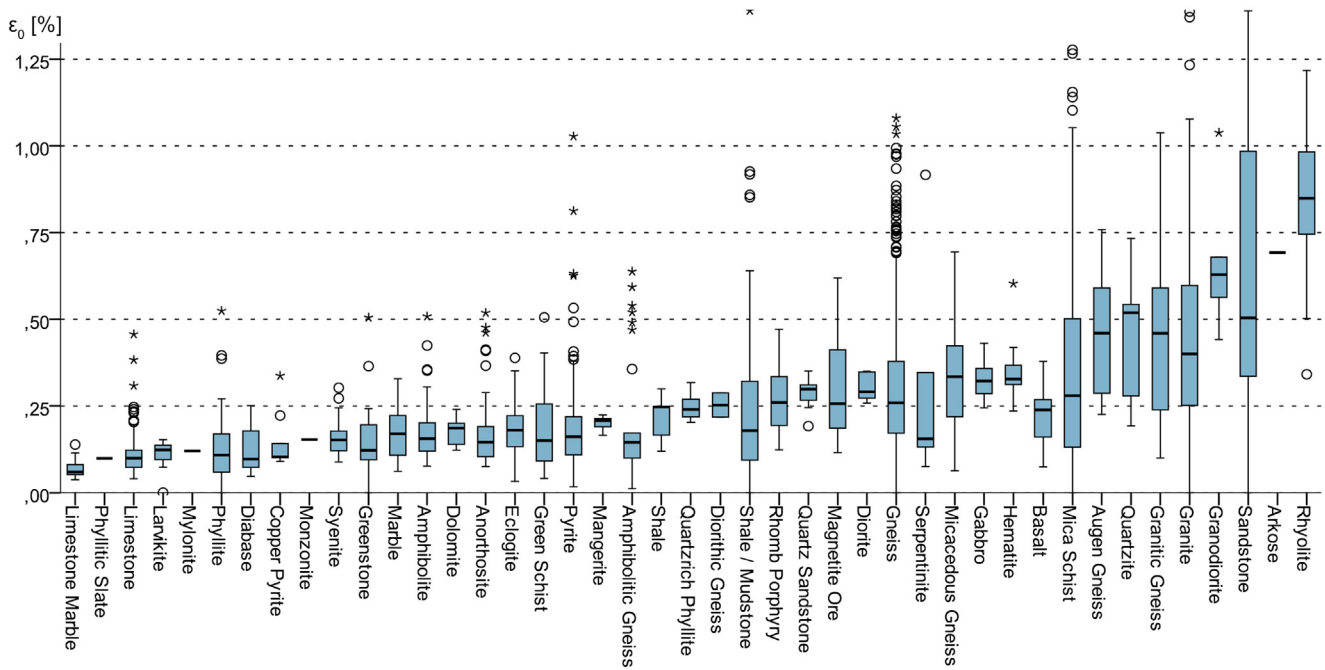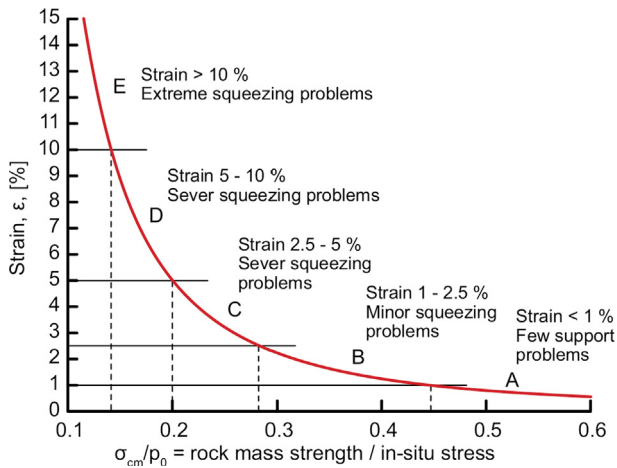support considerations. The plot shows only one case of a stability problem below the 1% line and it can also be seen that there are cases with as high as a 4% strain with no stability problems. For the different squeezing classes presented in Fig. 10, indications of the necessary support are provided: (A) bolts and sprayed concrete, (B) sometimes lattice girders or steel sets, (C) heavy steel sets, (D) fast installation and face support, and (E) yielding support may be required.

According to Hoek (1999), it is reasonable to assume an isostatic stress field, as in the Monte Carlo simulation done for Fig. 10, for very weak rock, such as in a fault or shear zone, since this type of rock has undergone failure and is incapable of sustaining significant stress differences. Because of this, even if the far field stresses are anisotropic, the stresses within the fault zone are likely to be approximately isotropic.

3.4. Rock mass quality

In rock engineering, there are many tools for describing rock mass quality. These tools are often also used for designing support,
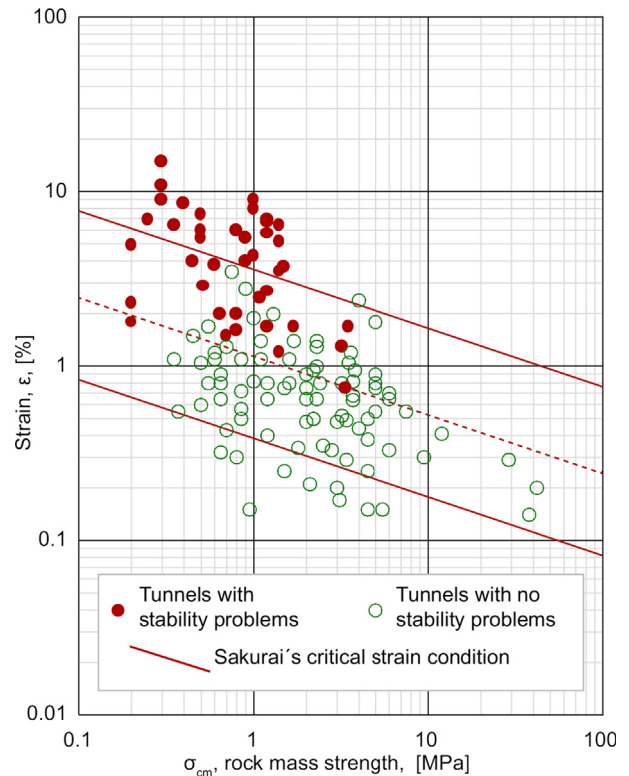
Fig. 11. Field observations from the Second Freeway, Pinglin and New Tienlun headrace tunnels in Taiwan, based on Hoek (2001), Hoek (1999) and Sakurai (1983).

evaluating alternative excavation methods or estimating input for rock engineering applications (Palmstrom and Stille, 2007). The tool that is used most by far in Norway is the Q-system. The Q-system is used for rock mass quality documentation and as a basis for support design, either with the "built-in" support chart (e.g. the rail authorities (Bane NOR, 2018) or a modified chart defined by the road authorities (Statens vegvesen, 2016b). For engineering applications, the GSI (Hoek, 1994) is
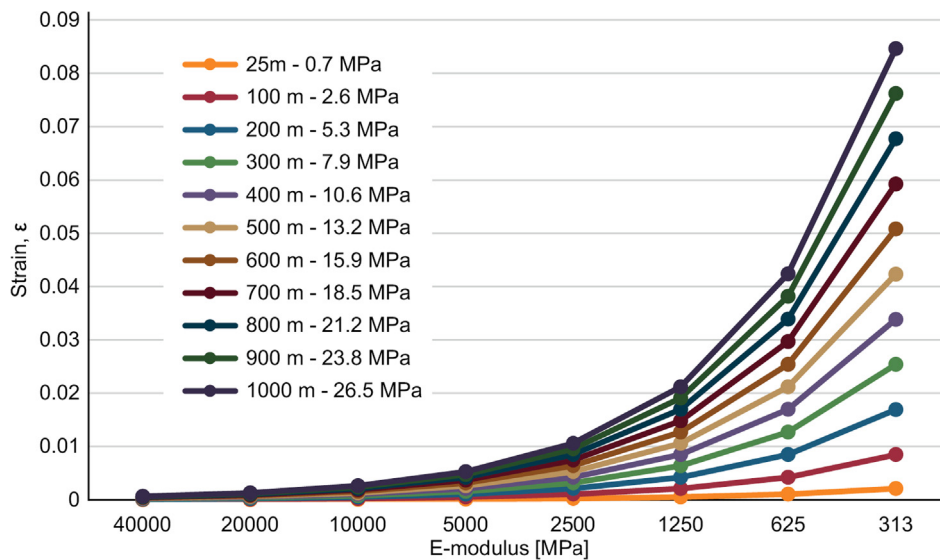
Fig. 12. Strain vs. E-modulus calculated based on Hooke's law for different (vertical) stresses.

usually used with the Hoek-Brown failure criterion and the rock mass E-modulus estimation (Hoek, 2006).

3.4.1. The Q-system

The Q-value is calculated from six parameters, as shown in Eq. (2) (Barton et al., 1974). The values for each parameter are extracted from tables, charts and/or equations based on mapping in the field or on cores. To visualize variations, one can take the minimum, maximum and mean value for each parameter and calculate Q-values. The Q-value is logarithmic and spans from 0.001 (exceptionally poor) to 1000 (exceptionally good).

$$Q = \frac{RQD}{J_n} \times \frac{J_r}{J_a} \times \frac{J_w}{SRF} \tag{2}$$

where RQD is the Rock Quality Designation.

J_n is the joint set number.
J_r is the joint roughness number.
J_a is the joint alteration number.
J_w is the joint water reduction factor.
SRF is the stress reduction factor.

RQD/J_n represents a description of block size, J_r/J_a represents the inter-block shear strength and J_w/SRF represents the active stress.

3.4.2. GSI

The Geological Strength Index was introduced in the mid-1990 s by Hoek and co-authors Kaizer and Bawden. The system provides a number that, when combined with the intact rock properties, can be used to estimate the reduction in rock mass strength for different geological conditions (Hoek, 2006).

The GSI can be estimated in-situ by using diagrams describing the structure and joint surface conditions. There are two alternative diagrams, one for blocky rock masses and one for heterogeneous rock masses. To obtain the GSI value or a range describing the rock mass, the rock structure and the surface of the discontinuities are combined in the appropriate diagram. The GSI value ranges from 0 to 100, where the higher value is the better rock mass.

One of the most recent contributions from the people behind the GSI is a quantification of the two sides of the GSI chart that makes it possible to calculate GSI values from parameter values registered with the Rock Mass Rating- (RMR) and Q-system. The structure (jointing) side of the diagram is replaced with RQD and the surface condition side is replaced with $JCond_{89}$ or the J_r/J_a from the Q-system. $JCond_{89}$ is a parameter from the RMR-system describing the surface conditions. See Eqs. (3) and (4) respectively for the two estimates (Hoek et al., 2013). An important aspect regarding these formulas is that they do not convert from one rock mass classification system to another directly as conversions have done before, but are based on using corresponding parameter registrations of the systems to calculate a GSI value as an alternative or supplement to using the charts.

$$GSI = JCond_{89} + RQD/2 \tag{3}$$

$$GSI = \frac{52J_r/J_a}{(1 + J_r/J_a)} + RQD/2 \tag{4}$$

3.5. The elastic properties of rock mass and weak rock

To estimate the E-modulus of the rock mass (E_{rm}), at least 15 different formulas have been proposed by different authors based on input of different rock mass quality parameters, such as Q, RMR and GSI (Aksoy et al. 2012; Palmström and Singh 2001; Hoek and Diederichs 2006). Most of these estimates are based on a limited amount of data (Hoek and Diederichs, 2006).

Hoek and Diederichs (2006) have proposed two equations that can be used with the GSI, based on a new dataset of almost 500 tests. In addition to an equation proposed earlier (Hoek et al., 2002), these equations are probably the most commonly used today because they are well documented and easy to use based on computer software. The three respective equations of E_{rm} have slightly different input parameters to suit different premises:

- *Generalized Hoek & Diederichs (2006)*, which considers the elasticity of intact rock (E_i), blast damage (D) and GSI;
- *Simplified Hoek & Diederichs (2006)*, which considers D and GSI; and
- *Hoek, Carranza-Torres, Corkum (2002)*, which considers the strength of intact rock (σ_{ci}), D and GSI.

Elastic strain can be calculated based on Hooke's law. To illustrate the relation between the three parameters, different probable values of stress, strain and E-modulus have been plotted in Fig. 12. Vertical stresses representing overburdens from 25 to 1000 m is used, where 0.7 MPa represents the gravitational stress at 25 m, 2.6 MPa for 100 m and the following stresses represent each subsequent even 100 m. The E-modulus ranges from 40 000 MPa to 313 MPa, where the high value represents e.g. a massive gneiss and the lowest value represents e.g. a

crushed, clayey weakness zone material. The plot merely shows the sensitivity of the deformation with respect to the E-modulus in different relevant stress states and must not be confused with actual strain in the tunnel.

As shown in Fig. 12, the E-modulus and stress have a far greater impact on strain on the right side of the plot, where the rock is weak with low E-values, than on middle and high E-values. At the same time, the strain for low stresses that represents shallow tunnels is very small, even with low E-values.

According to ISRM (1978), a rock is weak when the uniaxial compressive strength is below 25 MPa. Hoek (1999) had a bit more complex definition based on including the in-situ stress as well. He suggested that a rock is weak when the uniaxial strength is about one-third of the in-situ stress acting upon the rock mass. The value (one-third) is related to point 0.3 on the x-axis in Fig. 10, where the plot shows a sudden increase in convergence at about this point. This approach implies that the "weakness" of the rock is not only defined by the rock mass strength, but also by the stress conditions of the rock mass in which the tunnel is excavated.

As the weakness of rock also depends on the stress state, an upper limit of the E-modulus of weak rock is hard to define, but it may be easier to define a lower limit. One reasonable assumption might be that rock mass with E_{rm} close to soil should be considered weak rock. As an indication of what this lower limit may be, Bowles (1997) and Zhu (2012) have found E-values of about 50–200 MPa for dense clays and sands.

3.6. Rock stress

The in-situ stresses in the rock mass are usually defined by a gravity-driven vertical stress and a horizontal stress that is a ratio of the vertical, as shown in Eqs. (5) and (6).

$$\sigma_v = \gamma z \tag{5}$$

$$\sigma_h = k\sigma_v \tag{6}$$

Hoek (2006) referred to a large number of in-situ measurements which have shown that the ratio k tends to be high at a shallow depth and that it decreases with depth. Sheorey (1994) proposed an equation for k (see Eq. (7)) that is plotted in Fig. 13 for a selection of E-modules with the resulting stresses. The model is based on an elasto-static stress model of the earth and considers the elastic constants of the crust, density and thermal expansion. According to Hoek (2006), the estimated curves for k by Sheorey (1994) are similar to measured stresses published by Brown and Hoek (1978), Herget (1988) and others, and are therefore considered a reasonable basis for estimating the value of k.

$$k = 0.25 + 7E\left(0.001 + \frac{1}{H}\right) \tag{7}$$

4. Numerical parameter analysis of a typical two tube tunnel

The degree of deformation is essential when selecting support. In this includes the important decision regarding reinforcing support versus load-bearing support, in Fig. 10 shown as the switch/transition between the two represented by class B support. As discussed in Section 1 the arched RRS is considered a load-bearing support while unarched RRS has a more reinforcing effect. Two parameter studies with the aim to illustrate the deformations that can be expected with different stresses and rock qualities, and the effect of the zone width, have therefore been conducted to evaluate the conditions of where one need load-bearing support and where reinforcement may be adequate.
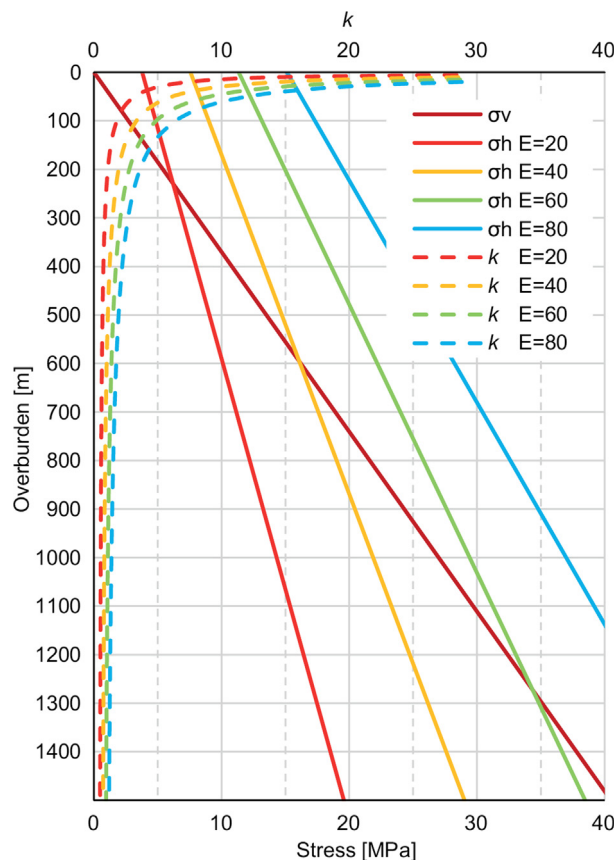

Fig. 13. The ratio k and calculated stresses toward depth, based on Sheorey (1994).

4.1. Influence of rock mass quality and stress on deformations

To investigate the relationship between stress and rock quality, numerical modelling was performed by using RS2 software (Rocscience Inc., 2017a). The model has two 10.5-m wide and 8-m high tunnels with 9.5-m rock between them, as shown in Fig. 12. Analysis was performed for 11 different overburdens, ranging from 35 to 1000 m. For 35-, 100- and 200-m depths, the horizontal and vertical stresses were applied as suggested by Sheorey (1994) for rock mass with E-modulus 20 GPa, as this was the most applicable model. From 300 m and further down, the horizontal stress was set equal to the vertical stress, which was gravitational, to avoid a horizontal stress that was lower than the horizontal. Stresses $\sigma_v = \sigma_h$ were input as suggested by Hoek (1999) for very weak rock, which is also of most interest in the study and has the most impact on deformations. This also conforms to the line drawn by Myrvang (1993) when he stated that vertical stress coincides well with overburden stress and is, at least at a depth down to 500 m, often the minor principal stress. The model is 1000 m wide with restraints in the x-direction of the vertical boundaries, restraints in the x- as well as y-direction at the bottom and no restrictions at the top. The tunnels were placed 37 m from the bottom of the model for all depths.

Parameters representative of quite a strong rock type, $\sigma_{ci} = 125$ MPa, $E_i = 20$ GPa and $m_i = 28$, were used as a basis for the rock mass parameter calculations. The rock parameters were adjusted for GSI values between 80 and 10, in intervals of 10, using the RocData software (Rocscience Inc., 2015a). *Generalized Hoek-Brown* was used as the strength criterion and *Generalized Hoek-Diederichs (2006)* was used for rock mass E-modulus (E_{rm}) estimation. The values for E_{rm} and in-situ rock stress used in the parameter study are shown in Tables 1 and 2.

A plastic analysis was performed based on an ideally elastic-plastic material. Generalized Hoek-Brown was used as a failure criterion. The

Table 1
Main material properties for numerical modelling.

GSI	E_rm [Mpa]	m_b
80	17,607	13.7
70	14,656	9.6
60	10,400	6.7
50	6144	4.7
40	3193	3.3
30	1628	2.3
20	913	1.6
10	610	1.1

Table 2
Vertical and horizontal rock stresses at tunnel depth in the different models.

Overburden	σ_v [Mpa]	σ_h [Mpa]
35	0.9	4.1
100	2.7	4.8
200	5.4	5.9
300	8.1	8.1
400	10.8	10.8
500	13.5	13.5
600	16.2	16.2
700	18.9	18.9
800	21.6	21.6
900	24.3	24.3
1000	27.0	27.0

Table 3
RRS-classes in the Q system. Ex. D45/6 + 2 Ø16-20, Si = single rebar layer, D = double rebar layer, 45 = thickness in cm, 6 + 2 = 6 rebar in first layer, 2 in second, Ø16-20 = rebar diameter in mm. (NGI, 2015).

RRS class	5-m span	10-m span	20-m span
I		Si30/6 Ø16–Ø20	D40/6 + 2 Ø16-20
II	Si35/6 Ø16-20	D45/6 + 2 Ø16-20	D55/6 + 4 Ø20
III	D40/6 + 4 Ø16-20	D55/6 + 4 Ø20	Special consideration

Fig. 14. Calculated deformations for a section of the model with a 500-m overburden and GSI 20. The deformations propagate far into the rock mass and the top displacement value is 50 m above the tunnel roof.

model had two stages, "initial" and "excavation", and the displacements were set to zero before "excavation" to ensure that only displacements from the excavation were registered.

In Fig. 14, results for the model with a 500-m overburden and the GSI 20 material from the parameter study are shown as an example. The reported displacement values from all models are the maximum value in the left tube, marked in the example with a " + ". The small difference between the tubes is due to the graded asymmetrical mesh.

Fig. 15 shows the results of the parameter study. The colours in the figure represent the different squeezing classes (Hoek, 2001), shown in Fig. 10:

- Green area represents no squeezing, sprayed concrete and rock bolts are described for support
- Orange represents minor squeezing, where you may need to add light lattice girders
- Red represents severe squeezing, where steel sets are recommended and you need to start to support the face
- Purple represents very severe squeezing, where forepoling, face reinforcement and steel sets are usually necessary

The results from the parameter study show that even very weak rock mass can be self-bearing using bolts and sprayed concrete for reinforcement, if the stresses are not too high. In the next section, which considers the impact of zone width, this tendency is shown to be even more distinctive for weakness zones with a potentially large reduction of deformations.

Basarir (2008) has done a similar study based on the Rock mass rating system (RMR) for a circular tunnel with overburdens from 100 to 500 m and studied how different rock support pressures affect the deformations. The results from this study are generally comparable to the results shown in Fig. 15. In addition, simple simulations using Roc-Support software (Rocscience Inc., 2015b) that uses an analytical approach yielded comparable values.

4.2. Influence of zone width on deformations

A 2D model like the one used in the parameter study above calculated as if the material extends infinitely in and out of the screen/paper-plane. In Fig. 14, where the displacements for the model with 500 m overburden and GSI 20 are shown, one can see that the displacement propagates far into the rock mass. In that case, when one is interested in the behaviour of weak rock that appears as faults/weakness zones, one loses the possible restraint from stronger rock when the displacement extends further than where the stronger rock is probably present.

To show the effect of weakness zone width, two main models with 100- and 500-m overburden, and the same tunnel geometry as the 2D models, were created in the 3D numerical software RS3 (Rocscience Inc., 2017b). The models are 150 m in the tunnel direction and 500 m wide. In the middle of the models, a material with weaker rock mass properties than the surrounding rock is used as a weakness zone. The weakness zone is perpendicular to the tunnel direction and different models with zone widths of 50, 25, 10, 5, 2.5 and 1 m were made. See Fig. 16a for an example of the model. The materials were copied from the 2D model, where the surrounding rock is the material properties for GSI 80 and the weakness zone GSI 20 (see Table 1). In addition, the restraints, failure criterion, stresses, etc were the same as for the 2D model.

To illustrate the distribution of displacement, a profile section of the middle of the zone and a longitudinal section along a tunnel tube for the 100-m overburden and 25-m zone width is shown in Fig. 16b and c. The zone width results are presented in Figs. 17 and 18, which show that displacement is strongly affected by zone width. The measurements are done high in the left wall (max. displacement) for the 100-m overburden and in the crown for the 500-m overburden. As the curves in the two figures have an almost identical distribution, it seems that the
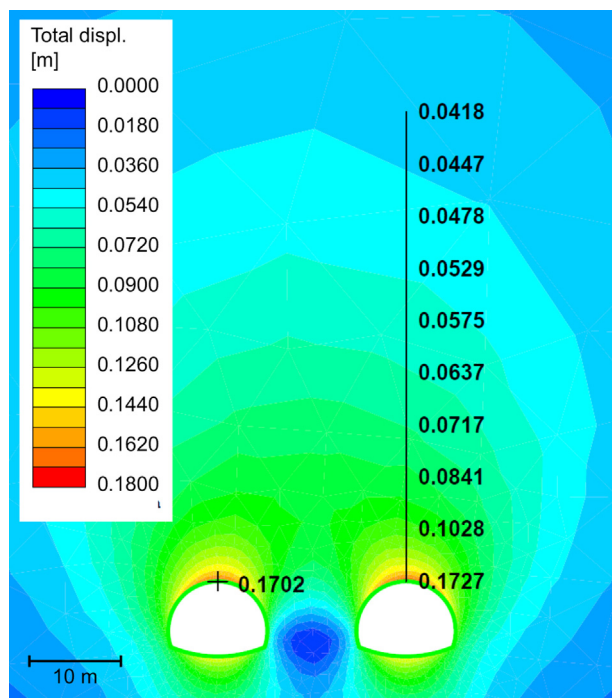
	GSI							
	80	70	60	50	40	30	20	10
35	2	2	3	6	11	23	43	74
100	2	2	3	6	11	22	40	69
200	3	3	5	8	15	31	60	106
300	4	5	7	12	23	48	92	170
400	6	7	9	16	32	66	131	249
500	7	8	12	21	40	85	170	340
600	8	10	14	25	50	106	227	451
700	10	12	17	30	60	130	271	585
800	11	13	19	34	69	148	315	696
900	13	15	22	39	80	174	370	857
1000	14	17	25	43	90	200	422	1030

(Left axis label: Overburden [m])

Fig. 15. Displacement in mm of a 10.5-m wide tunnel with different overburdens and rock mass qualities. Green is strain under 1%, orange between 1 and 2.5% and red above 2.5%. Fields with white text are the cases considered in the 3D model shown in Fig. 16 to Fig. 18. (For interpretation of the references to colour in this figure legend, the reader is referred to the web version of this article.)
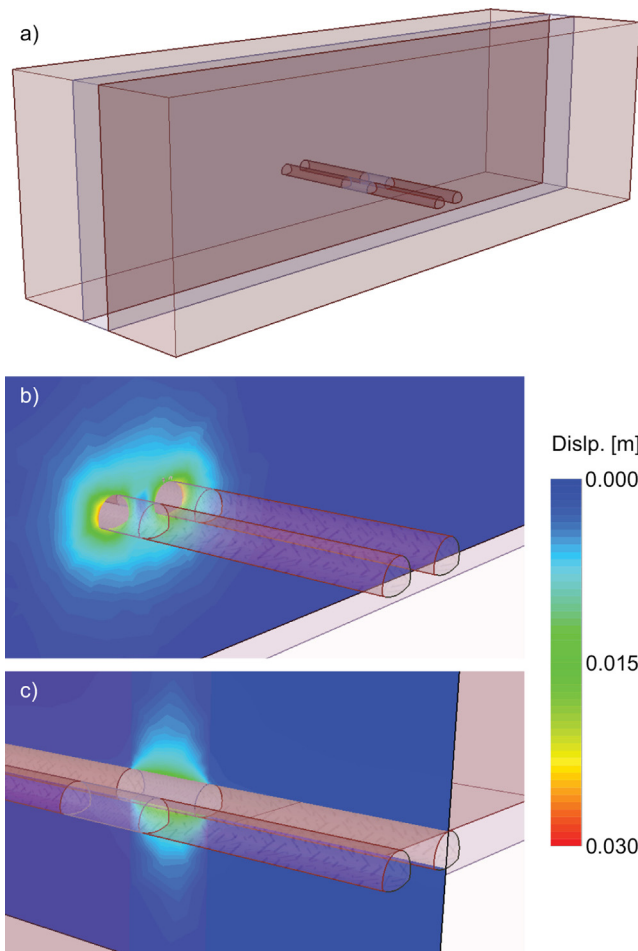

Fig. 16. 3D model with an overburden of 100 m and a weakness zone width of 25 m. (a) Model overview, (b) Profile section in the middle of the zone, and (c) Longitudinal section in the middle of the right tube.

Fig. 17. Maximum displacement along a 150-m long tunnel section with different zone widths, for an overburden of 100 m. The centre of the zone is at 75 m.

20), while for the 3D data and zone width of 1 m, the maximum displacement is 4 mm. For the 500-m overburden data, the 2D model yields a displacement of 170 mm, while the 3D data for a 1-m zone width is 17 mm and the 3D data for a 5-m zone width is 39 mm. This means that when the zone becomes smaller than approximately 5 m, the deformations have moved from the severe squeezing class to the no squeezing class.

5. Current support strategy for Norwegian road tunnels

As stated in Section 3.4, the Q-value is used for rock mass classification for road and railway tunnels in Norway. The rock support chart developed by the road authorities is largely based on the rock support

deformation for a certain zone width is strongly correlated to the deformation for a certain material/overburden combination (displacement values presented in Fig. 15). In looking at the 100-m overburden data, one can see that for the 2D data, representing an infinite zone width, the displacement is 40 mm (Fig. 15, overburden 100 and GSI
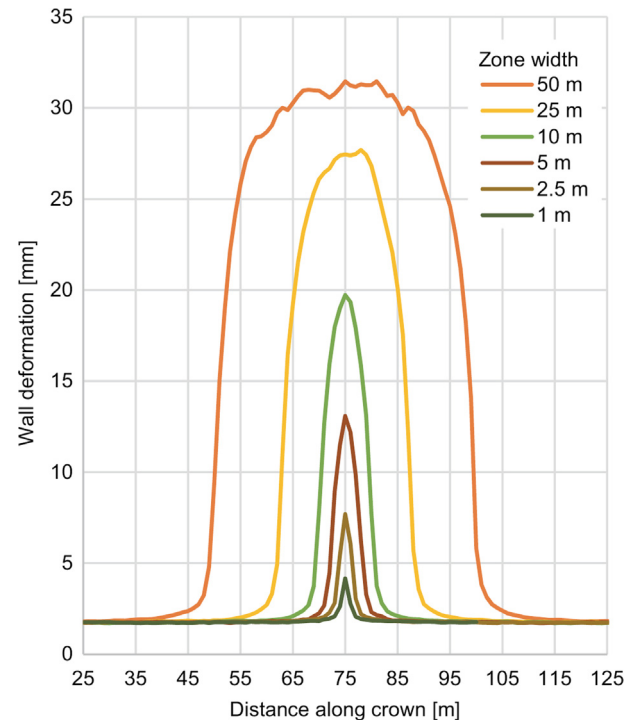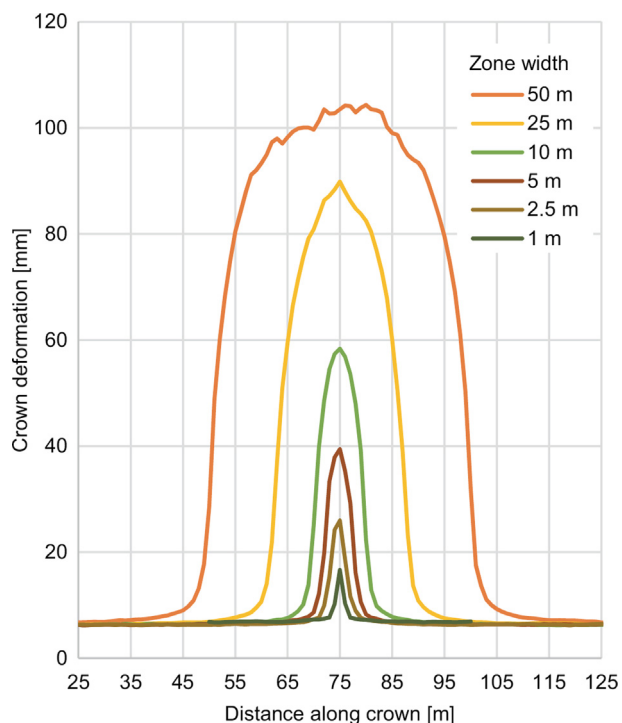
Fig. 18. Displacement at the crown along a 150-m long tunnel section, with different zone widths, for an overburden of 500 m. The centre of the zone is at 75 m.

chart in the Q-system (Pedersen et al., 2010) and the Q-system support chart is therefore also presented even if it is not directly used. The support strategy is subject to European design standards and the main principles from this standard are presented. In the discussion section, the current Norwegian support strategy will be debated and some possible changes will be suggested.

5.1. Rock support according to the Q-system

The Q-system support chart (see Fig. 19) is empirical when it comes to bolts and sprayed concrete, and mainly analytical regarding RRS. The support chart has been updated two times with about 2000 rock

support/Q-value cases since the original publication in 1974 (NGI, 2015). The background for the RRS dimensioning is given in Grimstad et al. (2002), and is based on arched RRS.

For estimation of rock support using the support chart a parameter called "Equivalent dimension" is introduced, which is the span or height of the tunnel divided by the Excavation Support Ratio (ESR). The ESR expresses the safety requirements and is used to adjust for different rock support needs e.g. for a temporary mine opening versus a road tunnel.

In the handbook (NGI, 2015) on using the Q-system, it is stated that spiling should be used for Q-values lower than 0.6 to 0.1 and that at a Q_m (mean value) of the Q-value can be used for support of narrow weakness zones. The handbook also pointed out that one should be aware of discontinuities that form wedges in the crown and walls, and that the direction and placement of the bolts must be considered according to these discontinuities.

5.2. Rock support for Norwegian road and railway tunnels

The Norwegian Public Roads Administration (NPRA) has developed its own support table specially fitted to road tunnels safety levels, tunnel dimensions and durability requirements, as shown in Table 4. It was implemented in 2010 and incorporated into NPRA regulations N500 road tunnels (Statens vegvesen, 2016b), with more extensive descriptions in the V520 Road tunnels manual (Statens vegvesen, 2016a).

The NPRA requires the application of the Q-system for mapping Q-value and has defined support classes that are related to the NGI rock mass classes. In the NPRA regulations, general requirements regarding pre-investigations, rock mass classification and mapping during construction are described. Excavation and support toward and through weakness zones, support effect, design and execution of RRS (arched) are also described. The recommended support is integrated with the drilling and blasting excavation cycle and the dimensioning is largely based on the Q-system support chart.

5.3. Design according to Eurocode 7

According to EU rules, geotechnical design shall be done according to NS-EN 1997–1 Eurocode 7: Geotechnical design (Standard Norge, 2008), which Norway is also required to follow as an EEA member. There are generally four different approaches described for designing
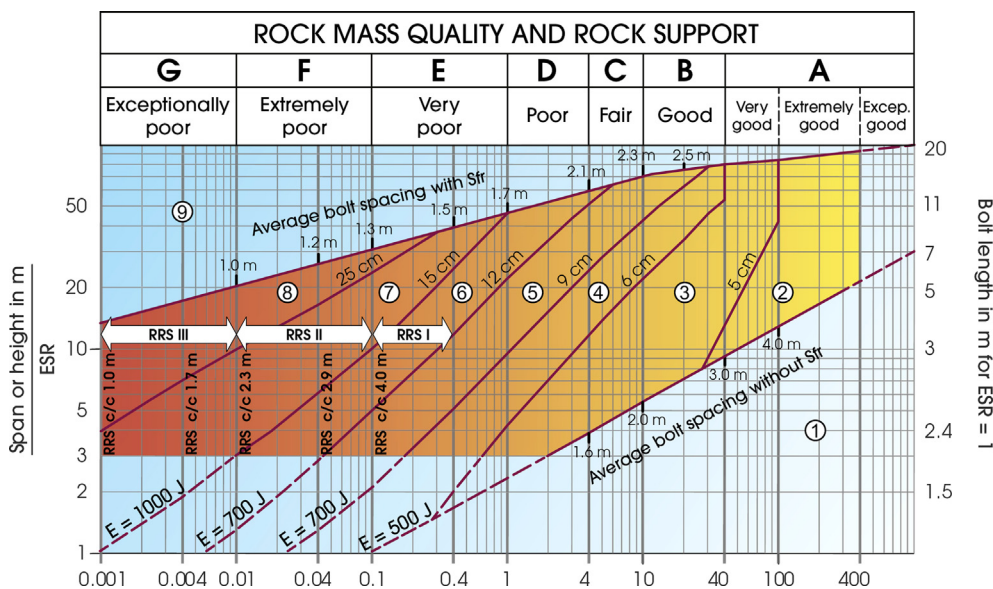

Fig. 19. The Q-systems rock support chart (NGI, 2015). For RRS dimensioning, see Table 3.

Table 4

Support table for Norwegian road tunnels developed by the NPRA (Pedersen et al., 2010; Statens vegvesen, 2016b).

Rock mass class	Rock conditions Q-value	Support class Permanent support
A/B	Weakly jointed rock mass Average joint spacing > 1 m. Q = 100–10	Support class I - Scattered bolting - Sprayed concrete B35 E700, thickness 80 mm
C	Moderate jointed rock mass Average joint spacing 0.3–1 m. Q = 10–4	Support class II - Systematic bolting, center/center (c/c) 2 m - Sprayed concrete B35 E700, thickness 80 mm
D	Strongly jointed rock mass or bedded schistose rock Average joint spacing < 0.3 m. Q = 4–1	Support class III - Sprayed concrete B35 E1000, thickness 100 mm - Systematic bolting, c/c 1.75 m
E	Very poor rock mass. Q = 1–0.2 Q = 0.2–0.1	Support class IV - Systematic bolting, c/c 1.5 m - Sprayed concrete B35 E1000, thickness 150 mm - Systematic bolting, c/c 1.5 m - Sprayed concrete B35 E1000, thickness 150 mm - RRS: Rib dimension E30/6 Ø20 mm, c/c 2 – 3 m, Bolting along arch c/c 1.5 m, length 3 – 4 m - Invert cast concrete must be evaluated
F	Extremely poor rock mass. Q = 0.01–0.1	Support class V - Systematic bolting, c/c 1.0–1.5 m - Sprayed concrete B35 E1000, thickness 150–250 mm - RRS: Rib dimension D30/6 + 4 Ø20 mm, c/c 1.5–2 m Bolting along arch c/c 1.0 m, length 3–6 m Can be replaced with lattice girders - Invert cast concrete, pitch min. 10% of tunnel width
G	Exceptionally poor rock mass Q < 0.01	Support class VI - Excavation and support design to be evaluated for each case

and dimensioning:

- Design by calculation
- Design by prescriptive measures
- Load tests and tests on experimental models
- Observational method

The most relevant approaches for Norwegian tunneling are prescriptive measures and the observational method. Prescriptive measures can be used e.g. if calculation models are not available. The measures should involve conventional and generally conservative rules in the design, and the strategies described in the two previous sections are usually associated with this approach.

The observational method is to be used e.g. if the prediction of the geotechnical behaviour is difficult. The main principle of this approach is to monitor, control and, if required, review or modify the design during construction. A typical approach is to have a monitoring strategy and a plan with established limits of behaviour and actions if the limits are exceeded.

The observational method is typically an alternative if one expects rock mass qualities of e.g. class G in Table 4, where an evaluation for each case is described. In the Frøya Tunnel, a case which will be discussed in some detail in Section 6.3, this principle was applied. The observational approach is also to a certain extent the basis for the New Austrian Tunneling Method (NATM), which is based on qualitative ground condition descriptions associated with excavation techniques and standard rock support requirements, with the rock as the essential load-bearing element. During and after excavation, the deformations are monitored to assess the stability of the tunnel (Maidl et al., 2013; Palmstrom and Stille, 2007).

Numerical modelling is commonly used as a tool for investigating the deformations, stresses and effects of rock support in more complex rock engineering conditions. The quality of input parameters is of great importance and if numerical modelling is used in the design of a specific case, one should always perform measurements during construction to verify the calculations.

6. Characteristics of rock mass quality, support and deformations in Norwegian road tunnels

In the following three sub-sections, data on the rock mass and support of present tunnels and deformation measurements performed in Norwegian tunnels will be presented. In addition, a case example of Norwegian road tunnel support from before the implementation of the NPRA support chart will be provided.

6.1. Rock cover, GSI and rock support

Since 2010, continuous registration of geology and rock support during excavations of Norwegian road tunnels has been mandatory, and the data have to be registered in a system called Novapoint Tunnel. After an excavation is completed, the data are stored in a national tunnel database. In addition, the tunnel geometry and terrain surface are stored in the system making it possible to connect rock mass quality and overburden by chainage numbers. Currently there are data for 38 tunnels in the database.

For each blasting round during excavation, the Q-value and its six parameters are registered. These Q-values have been exported to Excel for all tunnels registered in the database. In addition the overburdens for the same tunnels have been exported and combined with the rock mass properties of each tunnel in Excel. All tunnels have then been imported into the statistics software SPSS (IBM Corp., 2013), resulting in a data set with about 14 000 cases, with each representing a Q-value/blast round and yielding a tunnel length of 85 km all together.

A GSI value has been calculated for each blasting round based on Eq.4. In Fig. 20 the tunnel lengths for different GSI values and

					GSI						Tunnel m
		90	80	70	60	50	40	30	20	10	
Overburden [m]	0-35	52	1805	3156	5172	4884	2391	815	78	22	
	35-100	33	2654	4627	4932	4491	1999	444	146	0	
	100-200	25	2098	5559	4867	1929	546	98	38	0	
	200-300	0	1152	2862	2721	1148	155	16	24	0	
	300-400	0	962	2265	2766	839	284	72	23	22	
	400-500	11	1027	1528	1858	517	84	47	23	0	
	500-600	10	1016	1291	566	237	104	13	15	0	>2500
	600-700	0	415	222	101	50	5	0	0	0	2500-250
	700-800	0	562	97	41	0	0	0	0	0	250-50
	800-900	31	1318	160	0	0	0	0	0	0	<50
	900-	0	0	0	0	0	|0	0	0	0	

Fig. 20. Total tunnel meters excavated for 38 Norwegian road tunnels sorted according to GSI values and overburden. The green line marks the transition where the deformation according to Fig. 15 exceeds 1%, with > 1% to the right of the line. (For interpretation of the references to colour in this figure legend, the reader is referred to the web version of this article.)

					GSI						Support classes
		90	80	70	60	50	40	30	20	10	
Overburden [m]	0-35					15	50	206 / 20	15 / 35	22	
	35-100					5	13	40 / 5	83 / 30		
	100-200						3	38	2		
	200-300							10	24		
	300-400								4	6 / 16	
	400-500						11	5	23		
	500-600								15		
	600-700										IVb
	700-800										V
	800-900										VI
	900-										

Fig. 21. Tunnel meters supported with arched RRS for different GSI values and overburden for the same data set as in Fig. 20. The green line marks the transition where the deformation according to Fig. 15 exceeds 1%, with > 1% to the right of the line. (For interpretation of the references to colour in this figure legend, the reader is referred to the web version of this article.)

overburden combinations are combined. As shown in the chart, the main weight is on relatively high GSI values (97.6% of the tunnel length is GSI 40 or above). Few cases have both low GSI value and high overburden.

Since the support class (shown in Table 4) corresponds to a certain Q-value interval for these tunnels, it is possible to sum up the length for a certain type of support. In Fig. 21, the use of arched RRS (classes IVb, V and VI) is shown for different combination of GSI and overburden. In Fig. 22, the total length for all support classes in the data set is shown. For example, one can see from Fig. 20 that 78 m of tunnel have been excavated in GSI 20 and with 0–35 m overburden, and from Fig. 21, that of these 78 m, 15 m have been supported with support class IVb and 35 m with V.

6.2. Deformation monitoring

It is not very common to monitor deformations during tunnel excavations in Norway. In Table 5, however, deformation measurements from six different tunnels are presented. For all tunnels except the Frøya tunnel, the measured sections are supported with arched RRS. For the

Frøya tunnel, which is discussed in more detail in Section 6.3, the measurements were used to evaluate the need for permanent support and the selection of different support measures. For the Rå and Sørås tunnels, very high swelling pressures were the main motivation factor for displacement surveillance.

As seen in the table, most deformations are very small with values lower than 1 mm. The largest values are approximately 20 mm. In considering the data, one must bear in mind that most measurements were done well behind the face and that rock reinforcement or support were already installed. The data will be further analysed in the discussion chapter.

Since the displacements in Table 5 are from zones where deformation for many of these were actively attempted to be stopped by installing load bearing support, it will not be relevant to compare these values with the displacements in Fig. 15, which are for unsupported rock mass and "infinite" zone width.

6.3. Case example: The Frøya tunnel

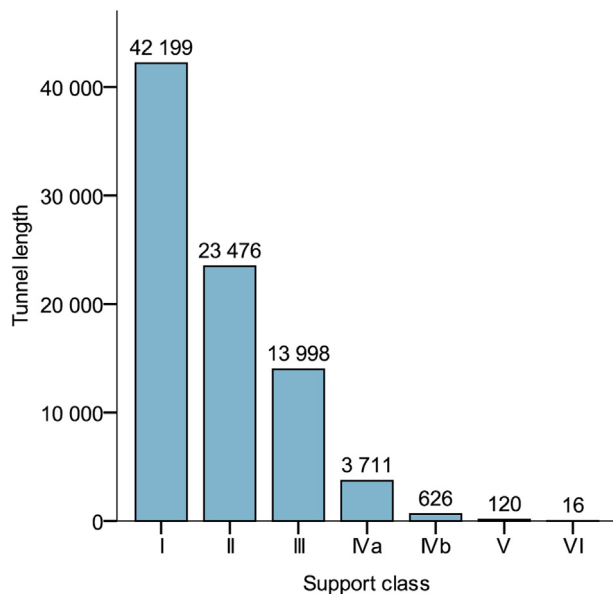The Frøya tunnel is a subsea road tunnel situated in Central Norway.

Fig. 22. Tunnel length and support measures for each class shown in Table 4.

The tunnel, which opened in the year 2000, has two lanes, a total length of 5300 m and its lowest point is 165 m below sea level. Geological pre-construction investigations indicated sections with very difficult rock conditions. An extensive follow-up arrangement was therefore designed, including continuous probe drilling, geological mapping, detailed registration of Q-values, deformation measurements and training for cave-in scenario. The mapped Q-values show that 1160 m of the tunnel were excavated in rock mass class E, 480 m were excavated in rock mass class F and 95 m were excavated in rock mass class G. As shown in Table 5, considerable time-dependent deformations were recorded during construction. According to the construction documentation, a large number of clay-rich weakness zones containing swelling clay were encountered (Statens vegvesen, 2000).

The Q-system rock support chart was not directly utilised during excavation, but comparisons between actual rock support and recommended support based on Q-values were conducted during excavation. Where large deformations could be expected, the deformations were measured using tape extensometers, and the recorded deformations were used as a basis to decide the final support.

Based on the recorded Q-values and rock support registered in Excel and as maps during construction, a dataset was produced in SPSS (IBM Corp., 2013) for this paper, systemizing the rock mass quality and the support for each tunnel meter.

To make the data more presentable, some categorizing was performed. For the plots in Fig. 23, the most extensive support for a tunnel meter determined the category. This means e.g. that a tunnel meter presented as RRS or cast concrete may also be supported with spiling. Some registrations in the transition between competent and weak rock have been omitted where heavy support has been used on a rock that was obviously too competent for this support. Invert cast concrete was used with all heavy support and excluded, as including it would double the number of categories.

An important point is that the RRS used in this project do not necessarily form a perfect arch but follow the blasted tunnel profile (un-arched RRS). This means that only the cast concrete can be regarded as rock support in the sense that it will be load-bearing; the rest must be considered rock reinforcement. A few lattice girders were used in the Frøya tunnel and registered in this study as cast concrete. For more details regarding the support, excavation methods and measurements, reference is made to Holmøy and Aagaard (2002).

In Fig. 23, the different support measures are plotted with respect to rock mass quality. An important point to keep in mind while reading

these diagrams is that consequences regarding the choice of support only can be observed with too little support, not too much. This means for instance that the use of cast concrete in the better part of the scale may not have been necessary, but the use of spiling in the poorer part of the scale actually worked. Some sections may also be over-supported in the transition between a "good" and "fair" rock and add the length of a more extensive support than necessary for the "good" rock.

As can be seen from the diagrams in Fig. 23, the weights of different support measures are arrayed in a reasonable order from light to heavy, with decreasing rock mass quality. It can also be observed that a considerable amount of bolt/sprayed concrete, spiling and RRS have been used as support in more or less all rock qualities. This indicates there may be factors that are not identified by the input parameter, but have a significant impact on the required support.

7. Discussion

In this section, the preceding theory and data will be discussed to consider the present use and potential need for changes of rock support recommendations for Norwegian tunnels, with a focus on deformations.

According to the critical strain concept, Norwegian hard rocks will have small deformations when they fail, and since they have high uniaxial compressive strength, they can withstand high rock stresses before that happens. The critical strain increases when considering rock mass compared to rock/cores, as shown by Sakurai (1983). Considering the reduction of E-modulus and uniaxial compressive strength for rock masses compared to rock mass quality, according to Hoek and Diederichs (2006) and Hoek et al. (2002), one can assume that the reduction in critical strain is also dependent on rock mass quality.

A relationship between rock mass strength and in-situ stress and the expected deformation of the tunnel was established by Hoek and Marinos (2000), as shown in Fig. 10. Based on their own and Sakurai's (1983) work, they stated that it seems a tunnel closure of 1% is a limit for where one needs to consider supporting the rock with more than bolts and sprayed concrete. Further, they stated that bolts and sprayed concrete may be sufficient even at up to 2.5% tunnel closure.

Fig. 15 shows that both quite a large overburden and a weak rock mass must be present to cause deformations that required more than bolts and sprayed concrete for rock support, according to the limits suggested by Hoek and Marinos (2000). The deformations presented from the parameter study suppose that the material parameters are constant along the tunnel axis. When the deformations are large, they propagate quite far out from the tunnel periphery. To show how a side rock of a better quality would affect the deformations, models with 100 and 500 m overburden were created in 3D, simulating a perpendicular weakness zone with GSI 20 of different widths with side rock of GSI 80 material. As shown in Figs. 17 and 18, the zone width has a substantial effect on the deformations, wherein a 10- and a 2.5-m wide zone at maximum only have about 60% and 25% of the deformation of the 50-m zone.

In Table 5, deformation measurements from some Norwegian tunnels are presented. The values are generally a few mm and the largest deformations are from the Frøya tunnel, with maximum values of approximately 20 mm. For the Frøya tunnel, measurements were done well behind the face and therefore only the "tail" of the total deformation was registered. Since the tunnel face was at least 30 to 60 m away from the measurement point, it is not probable that the tunnel advance was causing the deformations, but rather time-dependent squeezing/creep/swelling and stress redistribution. Practically all the zones in the tunnel contained swelling clay.

The rock in Norway, as shown in Figs. 4 and 5, is mainly strong (50–100 MPa) and very strong (100–250 MPa) and has E-modulus in the range of 25–50 GPa. The rock mass is usually of a quality that is easy to support, meaning bolts and sprayed concrete are sufficient. Of the total tunnel length of 84 100 m in the Norwegian tunnel database, only 760 m (< 1%) had a Q-value lower than 0.2, which implies the use

Table 5

Displacement measurement data from Norwegian road and railway tunnels. Positive values are inward movement in mm. GSI values are calculated based on Eq. (4). In the horizontal or vertical displacement column, measurements done with an extensometer are vertical while the rest are horizontal. The diagonal displacement columns are measured from the wall on one side of the tunnel to the spring line on the other side.

| Tunnel	Year	Method	Chainage	Hor or vert displ. [mm]	Diagonal displ. 1 [mm]	Diagonal displ. 2 [mm]	Instrument installation	Water/soil overburden [m]	Rock overburden [m]	Q-value	GSI
Finnfast subsea road tunnel	2008	Extensometer	12782.5	1.1			At face	50	90	0.010	10
Bærum railway tunnel	2007	Extensometer	1220	0.3			Before pass	3.5	4.5	0.44	49
Løren road tunnel (TA)	2010	Extensometer	1220	2.16			Before pass	26	7	2.5	47
Løren road tunnel (TB)	2010	Extensometer	1220	2.39			Before pass	23	7	1.0	49
Sørås road tunnel (T51)	2016	Conv., tot. stat.	13,171	1.2			face at 13,177		32	0.25	34
Sørås road tunnel (T51)	2016	Conv., tot. stat.	13,177	4.7	−2.6		at face		32	0.25	34
Rå road tunnel (T52)	2016	Conv., tot. stat.	13,250	0.6			face at 13,294		35	0.35	49
Rå road tunnel (T52)	2016	Conv., tot. stat.	13,532	0.6			face at 13,607		33	0.35	40
Rå road tunnel (T52)	2016	Conv., tot. stat.	13,602	2.3			face at 13,616		27	0.15	27
Frøya subsea road tunnel	1999	Convergence, tape	3440	13.50	0.65		30–60 m behind face		44	0.25	23
Frøya subsea road tunnel	1999	Convergence, tape	3992	0.70	4.40		30–60 m behind face	34	52	0.008	8
Frøya subsea road tunnel	1999	Convergence, tape	4003	0.45	1.68		30–60 m behind face	34	53	0.008	8
Frøya subsea road tunnel	1999	Convergence, tape	4012	0.75	3.09		30–60 m behind face	33	54	0.003	8
Frøya subsea road tunnel	1999	Convergence, tape	4820	0.39	−0.53		30–60 m behind face	25	121	0.19	23
Frøya subsea road tunnel	1999	Convergence, tape	5033	0.50	0.48		30–60 m behind face	34	114	0.13	18
Frøya subsea road tunnel	1999	Convergence, tape	5060	0.44	0.14		30–60 m behind face	32	117	0.19	23
Frøya subsea road tunnel	1999	Convergence, tape	5283	2.00	0.15		30–60 m behind face	31	120	0.18	24
Frøya subsea road tunnel	1999	Convergence, tape	5419	0.24	0.24		30–60 m behind face	41	112	0.13	25
Frøya subsea road tunnel	1999	Convergence, tape	5556	12.68	6.05	11.62	30–60 m behind face	50	104	0.20	27
Frøya subsea road tunnel	1999	Convergence, tape	5585	10.88	13.04	3.47	30–60 m behind face	55	101	0.15	23
Frøya subsea road tunnel	1999	Convergence, tape	6480	21.50			30–60 m behind face	36	100	0.025	13
Frøya subsea road tunnel	1999	Convergence, tape	6495	11.10	2.65	14.50	30–60 m behind face	36	100	0.017	11
Frøya subsea road tunnel	1999	Convergence, tape	6620	0.40	0.05		30–60 m behind face	24	104	0.10	18
Frøya subsea road tunnel	1999	Convergence, tape	6630	0.27			30–60 m behind face	24	103	0.050	21
Frøya subsea road tunnel	1999	Convergence, tape	6700	8.50	0.90		30–60 m behind face	24	101	0.11	24
Frøya subsea road tunnel	1999	Convergence, tape	6730	1.65	0.27		30–60 m behind face	24	100	0.042	16
Frøya subsea road tunnel	1999	Convergence, tape	6778	4.65	1.20		30–60 m behind face	24	98	0.33	28
Frøya subsea road tunnel	1999	Convergence, tape	6880	0.20	1.05		30–60 m behind face	25	91	0.027	15
Frøya subsea road tunnel	1999	Convergence, tape	6920	3.30	2.76	4.52	30–60 m behind face	25	88	0.013	10
Frøya subsea road tunnel	1999	Convergence, tape	6938	12.00	8.45	1.95	30–60 m behind face	25	88	0.050	17
Frøya subsea road tunnel	1999	Convergence, tape	7370	22.75	12.22		30–60 m behind face	22	61	0.022	16
Frøya subsea road tunnel	1999	Convergence, tape	7425	4.15	3.85		30–60 m behind face	21	57	0.008	8
Frøya subsea road tunnel	1999	Convergence, tape	7920	11.10	10.00		30–60 m behind face	.	31	0.015	10
Frøya subsea road tunnel	1999	Convergence, tape	8134	5.50	2.99		30–60 m behind face	.	19	0.15	29
Frøya subsea road tunnel	1999	Convergence, tape	8180	7.60	8.81		30–60 m behind face	.	16	0.25	28
Frøya subsea road tunnel	1999	Convergence, tape	8240	20.90	6.20		30–60 m behind face	.	11	0.13	23
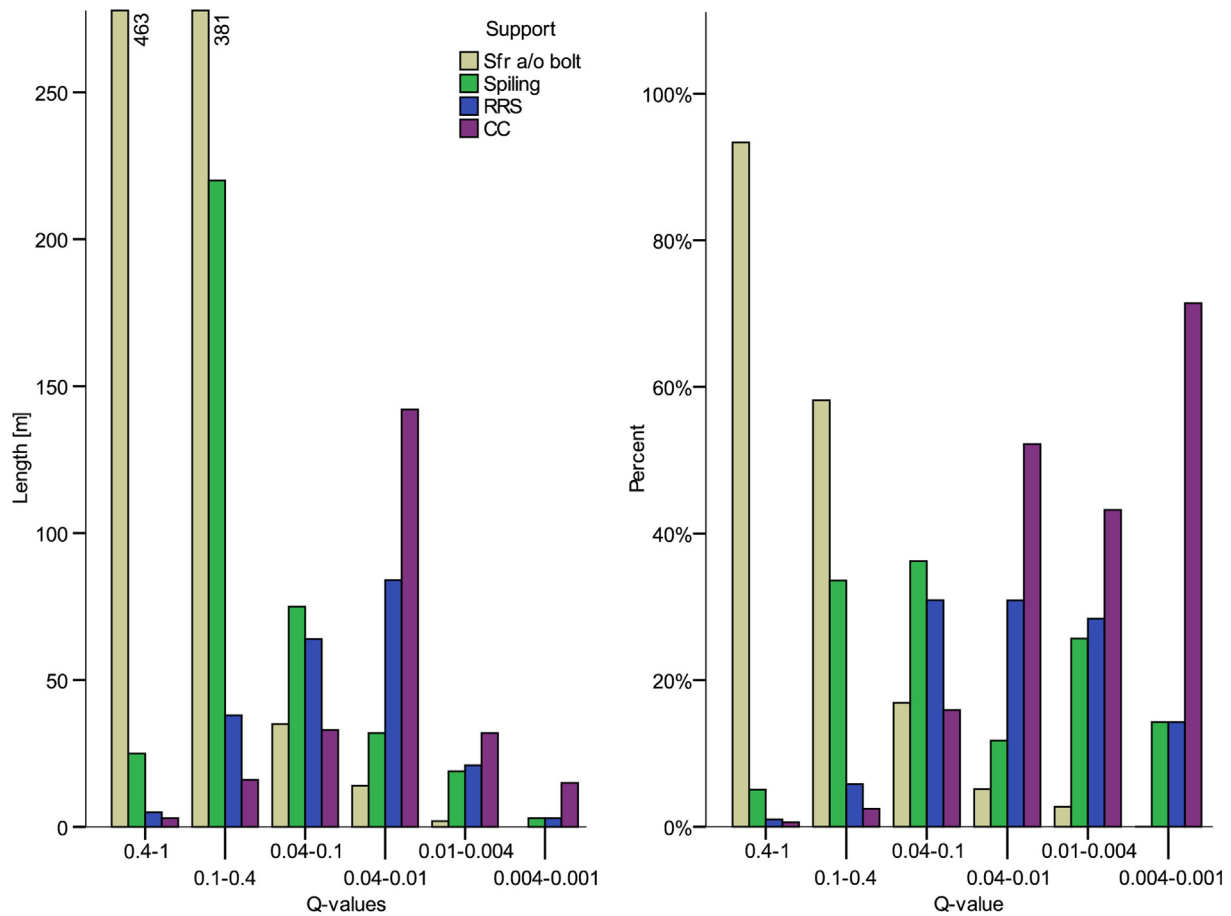
Fig. 23. Distribution of types of permanent support in weak rock in the Frøya tunnel. The diagram to the left shows the actual tunnel length supported with the different support measures and the diagram to the right shows the same information in percentages.

of arched RRS (see Fig. 22). As a comparison, the Frøya tunnel had 1230 m with Q-values lower than 0.2 of a total length of 5300 m and must be considered an extraordinary case.

The distribution of rock mass quality and overburden of recently opened tunnels in Norway is presented in Fig. 20. The axis of this figure has the same designation as Fig. 15. In considering the data in these figures, one can see that far most of the excavated tunnel length are in the green area where only small deformations are expected. If one in addition considers Fig. 15 one can see that most of the RRS is used in conditions that the parameter study suggests only reinforcement of the rock, not support. One should also have in mind that most of the weak rock appears in zones with the possible reduction that may give on the deformations.

Looking at the support data from the Frøya tunnel (see Fig. 23), where the Q-system support chart was not directly used, one can see that the different types of support overlap considerably in the different Q-value intervals. However, it seems that the support methods for each rock mass quality come in a reasonable order, ranging from lighter to heavier. But still, they do not effectively distinguish what type of support is needed for a certain value and it seems there must be processes that are not included by the input parameters in the Q-system but impact the necessary support, or that the parameter values are not weighted properly. To summarize, the rock mass that requires support for large deformations is not well distinguished from the rock mass that only requires reinforcement.

As shown in the parameter study, stress has a great influence on the expected amount of deformation and 3D analysis demonstrated that when a weak rock mass occured in a zone surrounded by more solid rock, the zone width had a significant impact on the deformation. The

Q-value is supposed to consider this through the SRF parameter, which is split into four categories: weakness zones (values 2.5–10), squeezing (values 5–20), swelling (5–15) and competent rock, including rock burst. A main issue is the value ranges. As seen in the parameter study and in Hoek and Marinos (2007) squeezing classes, the problems caused by deformations exist within a larger range than these values take into account. The SRF parameter considers input on both rock mass and stress, which is not favourable when used for support analysis, since it seems rock mass and stress should be handled separately in the more extreme cases.

Both the support chart for the Q-system (see Fig. 19) and the NPRA support table (see Table 4) describe arched RRS for the support of all weak rock mass from Q = 0.4 and Q = 0.2, respectively. This is also the limit where it is recommended that one start to use spiling bolts to keep the rock in place after blasting. For the Q-system, this limit is partly based on the data from the Frøya tunnel and one can see in Fig. 23 that they started to use spiling in the Q-value interval 0.4–0.1. As described for the Frøya tunnel above, spiling and non-arched RRS are used for all rock classes. On the basis of the parameter studies and the Frøya tunnel data, one can assume that these reinforcement measures are sturdy enough to avoid gravitational collapses due to cracked rock and unstable wedges, and also, to a certain degree, weakness zones containing swelling clay for cases with stresses expected reasonable near the surface.

As discussed in the section above, the deformations in Norwegian tunnels are generally very small. This also applies for weak rock mass that is not too far below the surface. For large deformations requiring load-bearing support to occur, an unfavourable combination of weak rock and stresses is required. Since it seems that the deformations

propagate far into the rock mass, the extent of the weak rock is also of significance for the actual deformations.

The literature suggests that a strain between 1 and 2.5% is the limit between the rock mass being reinforced and self-bearing to requiring support by load-bearing constructions. The currently most used system for rock mass classification and support decision making in Norwegian tunnelling does not seem to distinguish well between these two different concepts and describes load-bearing support for all weak rock, while it seems that for weak rock with reasonable stresses, reinforcement would be sufficient. The data showing rock mass quality with the overburden suggest that most of the constructed tunnel length by far belongs to the category where only reinforcement (bolts, sprayed concrete, spiling and unarched RRS) is required.

8. Conclusion

The introduction of RRS in the Q-value support chart and in the NPRA support table have caused a considerable increase in support in Norwegian road tunnels. If an effort had been made to identify under what conditions weak rock needs load-bearing support and under what conditions reinforcement is sufficient, a downscaling of heavy support for many tunnelling conditions would very likely be possible. A solution could be that for instance when the Q-value is below 0.4, one should also map the GSI. The GSI value could be considered with stresses and zone properties, such as width, heterogeneity and tunnel axis angle, to evaluate if a load-bearing construction is necessary and convergence measurements could be used to confirm support design.

The Frøya, Rå and Sørås are tunnels where large deformations were expected and/or one wanted extra safety margin. These tunnels, especially the Frøya tunnel, are examples of cases in Norwegian tunnelling where a more NATM-like approach was applied, using measurements for design and confirmation of design. With the use of total stations for convergence measurement, instead of the old tape extensometers, one could quite easily conduct more measurements than usual for Norwegian tunnelling to confirm stability. A systematic registration of measurements and rock mass properties could be used as background data for a potential new support dimensioning in weak rock.

Looking at the current dimensioning in Norwegian road tunnelling and based on the analyses and evaluations in this paper, it seems that support with arched RRS for all conditions below Q-value 0.2 is not necessary and a system that is more adapted to the actual deformation conditions should be considered.

References

Aksoy, C.O., Geniş, M., Uyar Aldaş, G., Özacar, V., Özer, S.C., Yılmaz, Ö., 2012. A comparative study of the determination of rock mass deformation modulus by using different empirical approaches. Eng. Geol. 131–132, 19–28. https://doi.org/10.1016/j.enggeo.2012.01.009.

Bane NOR, 2018. Technical regulations (Accessed 30.01.2018). < https://trv.jbv.no/wiki/Forside > .

Barton, N., Lien, R., Lunde, J., 1974. Engineering classification of rock masses for the design of tunnel support. Rock Mech. 6, 189–236. https://doi.org/10.1007/bf01239496.

Basarir, H., 2008. Analysis of rock–support interaction using numerical and multiple regression modeling. Canad. Geotech. J. 45, 1–13. https://doi.org/10.1139/t07-053.

Bowles, J.E., 1997. Foundation Analysis and Design, fifth ed. McGraw-Hill, Auckland.

Brown, E.T., Hoek, E., 1978. Trends in relationships between measured in-situ stresses and depth. Int. J. Rock Mech. Min. 15, 211–215. https://doi.org/10.1016/0148-9062(78)91227-5.

Carranza-Torres, C., Fairhurst, C., 1999. General formulation of the elasto-plastic response of openings in rock using the Hoek-Brown failure criterion. Int. J. Rock Mech. Mining Sci. 36, 777–809.

Duncan Fama, M., 1993. Numerical modelling of yield zones in weak rocks. In: Hudson, J.A. (Ed.), Comprehensive Rock Engineering. Pergamon, Oxford, pp. 49–75.

Grimstad, E., Kankes, K., Bhasin, R., Magnussen, A.W., Kaynia, A.M., 2002. Rock Mass Quality Used in Designing Reinforced Ribs of Sprayed Concrete and Energy Absorption, Bergmekanikkdagen. NFF, NBG, NGF, Oslo, pp. 39.31–39.19.

Herget, G., 1988. Stresses in Rock. Balkema, Rotterdam.

Hoek, E., 1994. Strength of rock and rock masses. ISRM News J. 2, 12.

Hoek, E., 1999. Support for very weak rock associated with faults and shear zones. International Symposium on Rock Support and Reinforcement Practice in Mining, Kalgoorlie, Australia.

Hoek, E., 2001. Big tunnels in bad rock. J. Geotech. Geoenviron. 127, 726–740. https://doi.org/10.1061/(ASCE)1090-0241(2001) 127:9(726).

Hoek, E., 2006. Practical Rock Engineering. < www.rocscience.com > .

Hoek, E., Carranza-Torres, C., Corkum, B., 2002. Hoek-Brown Failure Criterion – 2002 Edition NARMS-TAC Conference, Toronto, pp. 267–273.

Hoek, E., Carter, T., Diederichs, M., 2013. Quantification of the geological strength index chart. 47th US Rock Mechanics/Geomechanics Symposium. ARMA, San Francisco.

Hoek, E., Diederichs, M.S., 2006. Empirical estimation of rock mass modulus. Int. J. Rock Mech. Mining Sci. 43, 203–215. https://doi.org/10.1016/j.ijrmms.2005.06.005.

Hoek, E., Kaiser, P.K., Bawden, W.F., 1997. Support of Underground Excavations in Hard Rock, third ed. A.A. Balkema, Rotterdam.

Hoek, E., Marinos, P., 2000. Predicting Tunnel Squeezing Problems in Weak Heterogeneous Rock Masses. Tunnels & Tunnelling International Polygon Media Ltd, London.

Hoek, E., Marinos, P., 2007. A brief history of the development of the Hoek-Brown failure criterion. Soils Rocks 30.

Holmøy, K.H., Aagaard, B., 2002. Spiling bolts and reinforced ribs of sprayed concrete replace concrete lining. Tunnell. Underground Space Technol. 17, 403–413. https://doi.org/10.1016/S0886-7798(02)00065-2.

IBM Corp, 2013. IBM SPSS Statistics for Windows, 22nd ed. IBM Corp., Armonk, NY.

ISRM, 1978. Suggested methods for the quantitative description of discontinuities in rock masses. Int. J. Rock Mech. Min. 15, 319–368. https://doi.org/10.1016/0148-9062(78)91472-9.

Maidl, B., Thewes, M., Maidl, U., Sturge, D.S., 2013. Handbook of Tunnel Engineering I: Structures and Methods. Wiley, Hoboken.

Myrvang, A.M., 1993. Rock stress and rock stress problems in Norway. In: Hudson, J.A. (Ed.), Rock Testing and Site Characterization. Pergamon, Oxford, pp. 461–471.

Myrvang, A.M., 2001. Bergmekanikk. Norwegian University of Science and Technology, Department of Geology and Mineral Resources Engineering, Trondheim.

NBG, 1985. Ingeniørgeologi berg. Tapir, Trondheim.

NFF, 2008. Tung bergsikring i undergrunnsanlegg, Håndbok. Norsk forening for fjellsprengningsteknikk, Oslo.

NGI, 2015. Using the Q-System – Rock Mass Classification and Support Design. Norwegian Geotechnical Institute, Oslo.

Palmström, A., Singh, R., 2001. The deformation modulus of rock masses — comparisons between in situ tests and indirect estimates. Tunnell. Under. Space Tech. 16 (2), 115–131.

Palmstrom, A., Stille, H., 2007. Ground behaviour and rock engineering tools for underground excavations. Tunnell. Underground Space Technol. 22, 363–376. https://doi.org/10.1016/j.tust.2006.03.006.

Pedersen, K.B., Kompen, R., Kveen, A.T., 2010. Arbeider foran stuff og stabilitetssikring i vegtunneler, Teknologirapport. Norwegian Public Roads Administration, Oslo.

Rocscience Inc., 2015a. RocData, 5.006 ed. Rocscience Inc., Toronto.

Rocscience Inc., 2015b. RocSupport. Rocscience Inc, Toronto.

Rocscience Inc., 2017a. RS2, 9.025 ed. Rocscience Inc, Toronto.

Rocscience Inc., 2017b. RS3, 2.008 ed. Rocscience Inc, Toronto.

Sakurai, S., 1981. Direct strain evaluation technique in construction of underground opening. The 22nd U.S. Symposium on Rock Mechanics (USRMS). American Rock Mechanics Association, Cambridge, Massachusetts.

Sakurai, S., 1983. Displacement measurements associated with the design of underground openings. In: International Symposium on Field Measurements in Geomechanics Zurich, pp. 1163–1178.

Sheorey, P.R., 1994. A theory for In Situ stresses in isotropic and transverseley isotropic rock. Int. J. Rock Mech. Min. 31, 23–34. https://doi.org/10.1016/0148-9062(94)92312-4.

SINTEF, 2016. Rock Mechanic Properties of Rocks Tested in Sintef Rock Mechanics Laboratory. In: Infrastructure, S.b.a. (Ed.).

Standard Norge, 2008. Eurocode 7: Geotechnical design. Part 1: General rules, Eurocode 7: Geotechnical design. Part 1: General rules. Standard Norge Standard online, Lysaker.

Statens vegvesen, 2000. Sluttrapport for fastlandsforbindelsen Hitra Frøya. Statens vegvesen.

Statens vegvesen, 2010. Vegtunneler.

Statens vegvesen, 2016a. Tunnelveiledning. In: vegvesen, S. (Ed.), V520, Oslo.

Statens vegvesen, 2016b. Vegtunneler. In: vegvesen, S. (Ed.), N500, Oslo.

Zhu, T., 2012. Some Useful Numbers on the Engineering Properties of Materials. Department of Geophysics, Stanford University, California.